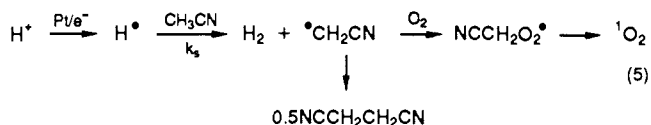


One may also consider the formation of solvent-derived radicals from a related sequence:

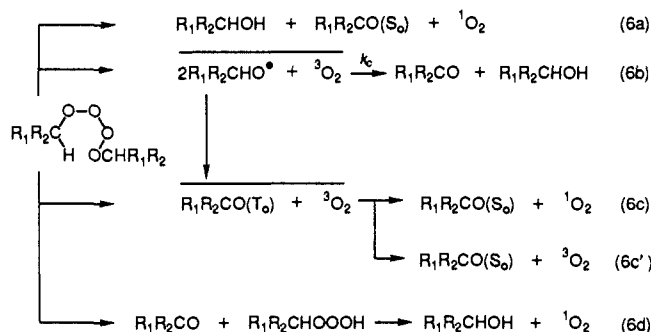


The partition of  $\text{H}^{\bullet}$  between solvent and oxygen will be given by

$$R = r(\text{}^{\bullet}\text{CH}_2\text{CN})/r(\text{}^{\bullet}\text{OOH}) = k_s[\text{H}^{\bullet}][\text{MeCN}]/k_0[\text{H}^{\bullet}][\text{O}_2]$$

Experimental values of  $k_s$ ,<sup>7</sup>  $k_0$ ,<sup>8</sup> and oxygen solubility<sup>9</sup> are known, from which we estimate values of  $R = 0.01$ – $0.2$ . Electrolysis of nitrogen-purged acetonitrile under the conditions described<sup>6,10</sup> gave a significant yield ( $9.0 \pm 0.9\%$ ) of succinonitrile.<sup>11</sup> The yield fell to  $0.5 \pm 0.2\%$  when the experiment was repeated while a continuous stream of oxygen was passed through the liquid. Experiments with oxygen-free solvent with anode and cathode compartments separated by a glass frit revealed succinonitrile in both compartments, consistent with the similar anodic oxidation of acetonitrile, described by Schmidt and Noack.<sup>12</sup> Since isotopic scrambling<sup>13</sup> of  $^{36}\text{O}_2$ – $^{32}\text{O}_2$  mixtures in autoxidizing media is well-established, we conclude that the mass spectrometric and other evidence presented<sup>6</sup> for reaction 4 must be tempered by a contribution from the concurrent reaction 5.

The product distribution from reaction 1 has been suggested to arise from spin conservation<sup>14</sup> in the fragmentation of a tetraoxide intermediate.<sup>15</sup> Some detailed pathways are as follows:



The  $^1\text{O}_2(^1\Delta_g)$  from diphenylmethane ( $11.3 \pm 0.6\%$ ) may reasonably arise from paths 6a, 6c, and 6d as shown. Our computer modeling of the stable products indicate that reaction 6b is not significant. The yield of  $^1\text{O}_2(^1\Delta_g)$  from quenching of triplet benzophenone by oxygen<sup>16</sup> has been measured as 29–35% and is too high to allow any combination of paths 6a and 6c in our system. The yield of triplet benzophenone from dismutation of alkoxy radicals<sup>17</sup> (vertical arrow between 6b and 6c above) is only 0.15%, too low to be a significant source of singlet oxygen.

Previously we suggested<sup>3</sup> that cleavage of  $\text{R}_2\text{O}_4$  into a carbonyl product and  $\text{ROOOH}$  might be a source of singlet oxygen when the hydrotrioxide decomposed (6d). This hypothesis appears to be ruled out by an experiment in which  $\text{Ce}^{4+}$  was injected into methanolic 1-tetralyl hydroperoxide (TOOH) at  $25^\circ\text{C}$  and then at  $-78^\circ\text{C}$ .<sup>18</sup> The prompt IR emission resulting from the self-reaction of  $\text{TOO}^{\bullet}$  in these experiments was comparable at both temperatures, whereas the known *tert*-alkyl hydrotrioxides are stable<sup>19</sup> at  $-78^\circ\text{C}$ .

Perhaps 6a gives largely  $^1\text{O}_2(^1\Sigma_g)$ ,<sup>14,20</sup> which partitions between  $^1\text{O}_2(^1\Delta_g)$  and  $^3\text{O}_2$ , a known process in the condensed phase.<sup>21</sup> This explanation nicely accounts for the relative independence of  $^1\text{O}_2(^1\Delta_g)$  yields on alkyl structure. In our system, any 760-nm emission, which could be ascribed to the  $^1\Sigma_g \rightarrow ^3\Sigma_g$  transition of molecular oxygen, must have a quantum yield below the detectable limit of about  $10^{-10}$ .

The relative uniformity of the  $^1\text{O}_2$  yields in reaction 1 may offer advantages in the study of hydrocarbon autoxidation.

**Acknowledgment.** This work was supported by 3M Co. and by Himont USA, Inc. We thank Dr. J. R. Kanofsky for helpful discussions of IR detection equipment.

(17) Quinga, E. M. Y.; Mendenhall, G. D. *J. Am. Chem. Soc.* **1986**, *108*, 474–478.

(18) Methanolic  $\text{Ce}(\text{NH}_4)_2(\text{NO}_3)_6$  (1.0 mL of 0.150 M) injected into 4.0 mL of 0.134 M TOOH. Both solutions were precooled for the reaction at  $-78^\circ\text{C}$ .

(19) (a) Pryor, W. A.; Ohto, N.; Church, D. F. *J. Am. Chem. Soc.* **1983**, *105*, 3614–3622. (b) Plesnicar, B.; Kovac, F.; Schara, M. *J. Am. Chem. Soc.* **1988**, *110*, 214–222.

(20) Bogan, D. J.; Celii, F.; Sheinson, R. S.; Coveleskie, R. A. *J. Photochem.* **1984**, *25*, 409–417.

(21) Klingshirm, H.; Maier, M. *J. Chem. Phys.* **1985**, *82*, 714–718.

### Synthesis Using Plasmid-Based Biocatalysis: Plasmid Assembly and 3-Deoxy-D-*arabino*-heptulosonate Production

K. M. Draths and J. W. Frost\*

Department of Chemistry, Purdue University  
West Lafayette, Indiana 47907

Received August 14, 1989

A plasmid-based approach to microbial whole cell synthesis of 3-deoxy-D-*arabino*-heptulosonates DAH and DAHP (Scheme 1) has been developed by exploiting the catalytic activity of transketolase, an enzyme that occupies a long-overlooked niche in aromatic amino acid biosynthesis. DAH and DAHP have been obtained with enzymatic synthesis<sup>1a,c</sup> and microbial whole cell synthesis.<sup>1a,b</sup> The levels (1 mM) of DAH and DAHP synthesized by microbial whole cells are significantly lower than those levels (10 mM) achieved with cell-free enzymatic synthesis.<sup>1a</sup> By localizing the genes encoding transketolase and DAHP synthase on a single plasmid, coupled enzyme catalysis (Scheme 1) utilized during multistep, immobilized enzyme synthesis<sup>1a</sup> is reconstructed within the confines of an intact microbe. The result is an *Escherichia coli* strain that synthesizes substantially elevated levels of DAH and DAHP.

The activity of DAHP synthase, which catalyzes the condensation of D-erythrose 4-phosphate and phosphoenolpyruvate to form DAHP (Scheme 1), is known to control the flow of carbon

(7) In water,  $k_s = 1 \times 10^5 \text{ M}^{-1} \text{ s}^{-1}$ ; Witter, R. A.; Neta, P. *J. Org. Chem.* **1973**, *38*, 484–487.

(8) In water,  $k_0 = 2 \times 10^{10} \text{ M}^{-1} \text{ s}^{-1}$  for  $\text{H}^{\bullet} + \text{O}_2$ ; Sweet, J. P.; Thomas, J. K. *J. Phys. Chem.* **1964**, *68*, 1363–1368.

(9) In acetonitrile,  $8.1 \times 10^{-3} \text{ M}$ ; Achord, J. M.; Hussey, C. L. *Anal. Chem.* **1980**, *52*, 601–602. We were originally influenced by a lower value: Bruckl, N.; Kim, J. I. *Z. Phys. Chem.* **1981**, *126*, 133–150. The concentration of oxygen of course may be depleted near the electrode surface.

(10) Conditions: 0.1 M 70%  $\text{HClO}_4$  in HPLC grade acetonitrile, Pt wire anode, Pt mesh cathode, 3.0 V, 4 mA, 27 h.

(11) GC analysis was carried out after neutralization with KOH, with a 25-m OV-17 capillary column programmed for 7 m at  $40^\circ\text{C}$ , then 10 deg/min to  $200^\circ\text{C}$  (HP 5830A gas chromatograph).

(12) Schmidt, H.; Noack, J. *Angew. Chem.* **1957**, *69*, 638. A referee suggested that  $\text{HO}^{\bullet}$  rather than the perchlorate radical was the active species.

(13) Bartlett, P. D.; Traylor, T. G. *J. Am. Chem. Soc.* **1963**, *85*, 2407–2710.

(14) See: Kellogg, R. E. *J. Am. Chem. Soc.* **1969**, *91*, 5433–5436 and references therein.

(15) (a) Russell, G. A. *Chem. Ind. (London)* **1956**, 1483. (b) Bartlett, P. D.; Guaraldi, G. *J. Am. Chem. Soc.* **1967**, *89*, 4799–4801. (c) Blanchard, H. S. *J. Am. Chem. Soc.* **1959**, *81*, 4548–4552.

(16) (a) Gorman, A. A.; Hamblett, I.; Rodgers, M. A. *J. Am. Chem. Soc.* **1984**, *106*, 4679–4682. (b) Redmond, R. W.; Braslavsky, S. E. *Chem. Phys. Lett.* **1988**, *148*, 523–529.

(1) (a) Reimer, L. M.; Conley, D. L.; Pompliano, D. L.; Frost, J. W. *J. Am. Chem. Soc.* **1986**, *108*, 8010. (b) Frost, J. W.; Knowles, J. R. *Biochemistry* **1984**, *23*, 4465. (c) Turner, N. J.; Whitesides, G. M. *J. Am. Chem. Soc.* **1989**, *111*, 624.

## Scheme I

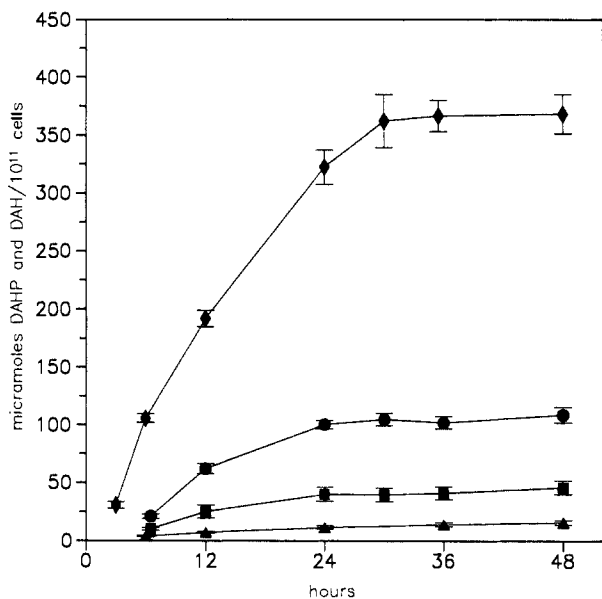
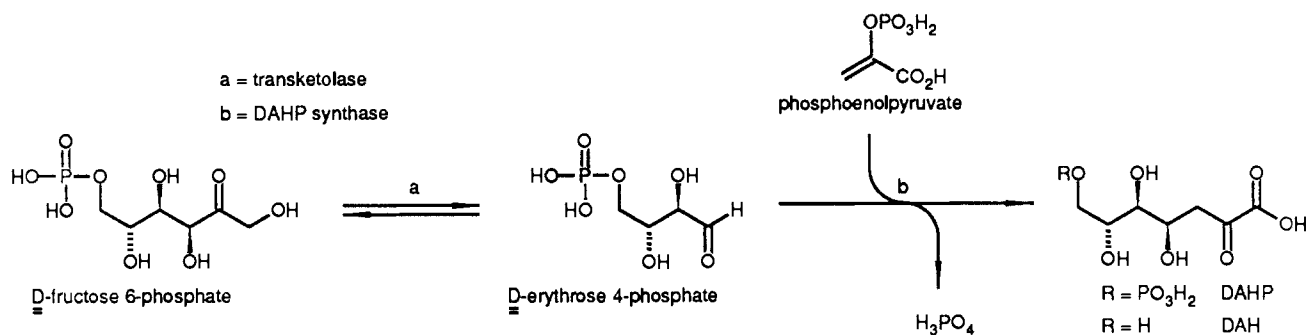
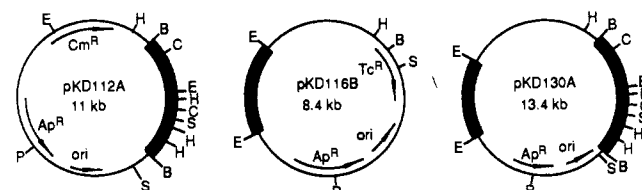


**Figure 1.** Micromoles (0–450) of DAH and DAHP per  $10^{11}$  cells produced by BJ502 *aroB* (▲), BJ502 *aroB* (pKD116B) (■), BJ502 *aroB* (pKD112A) (●), and BJ502 *aroB* (pKD130A) (◆) as a function of time (0–48 h). Colonies were inoculated into LB medium<sup>10</sup> containing kanamycin (0.05 g/L) or ampicillin (0.05 g/L) and grown at 37 °C for 12 h. Cells were harvested (time = 0), immediately resuspended in medium containing  $Na_3HPO_4$  (6.0 g/L),  $KH_2PO_4$  (3.0 g/L), NaCl (0.5 g/L),  $NH_4Cl$  (1.0 g/L),  $MgSO_4$  (0.12 g/L), glucose (2.5 g/L), shikimic acid (0.04 g/L), thiamine (0.001 g/L), and kanamycin or ampicillin, and returned to 37 °C incubation. Cell growth was monitored by optical density at 600 nm. A colorimetric assay<sup>7</sup> was used to determine DAH and DAHP levels.

into *E. coli* aromatic amino acid biosynthesis.<sup>2</sup> Introducing extrachromosomal copies of DAHP synthase encoding genes will increase the concentration of DAHP synthase, thereby increasing carbon flow into aromatic amino acid biosynthesis. Transketolase activity, as opposed to DAHP synthase activity, has not been considered a key component of aromatic amino acid biosynthesis.<sup>3</sup> Nonetheless, the amount of DAHP synthesized in *E. coli* could reflect the rate at which D-erythrose 4-phosphate is produced. Since transketolase catalyzes the interconversion of D-fructose 6-phosphate and D-erythrose 4-phosphate, DAHP synthesis may be influenced by increased transketolase activity resulting from expression of extrachromosomal transketolase-encoding genes.

To evaluate their impacts on microbial whole cell synthesis of DAH and DAHP, genes encoding transketolase and DAHP

## Scheme II



synthase were inserted into plasmid pBR325<sup>4</sup> (Scheme II). Plasmid pKD112A contained a 5-kb *Bam*HI insert encoding transketolase while pKD116B possessed a 2.4-kb *Eco*RI insert derived from the DAHP synthase *aroF* locus.<sup>5</sup> Both transketolase-encoding and DAHP synthase encoding genes were incorporated into plasmid pKD130A. Plasmids were individually expressed in the same host strain, *E. coli* BJ502 *aroB*, which extracellularly produces DAH and DAHP<sup>6,7</sup> due to the absence of the *aroB* gene product, dehydroquinate synthase. A 2.8-fold increase (Figure 1) in DAH and DAHP was synthesized by BJ502 *aroB* (pKD116B) relative to DAH and DAHP formed by BJ502 *aroB*. However, a much larger, 6.5-fold increase in DAH and DAHP was observed (Figure 1) when BJ502 *aroB* contained the transketolase-encoding pKD112A.

The largest increase (Figure 1) in extracellular accumulation of DAH and DAHP relative to BJ502 *aroB* is achieved with transketolase-encoding and DAHP synthase encoding plasmid pKD130A. Such an increase is consistent with the equilibrium nature of transketolase-catalyzed interconversion of D-fructose 6-phosphate and D-erythrose 4-phosphate. Even with additional intracellular transketolase activity, increased DAHP formation may not be realized if DAHP synthase activity is insufficient to couple D-erythrose 4-phosphate with phosphoenolpyruvate at a rate in excess of the rates at which the aldose phosphate is enzymatically and nonenzymatically converted into other products.<sup>8</sup> The importance of increasing the catalytic activity of DAHP synthase when increasing the activity of transketolase is reflected by the 23-fold increase of DAH and DAHP produced by BJ502 *aroB* (pKD130A).

Synthesis using plasmid-based biocatalysis endeavors to simplify access to small molecules which are normally difficult to obtain and to produce these molecules in quantities suitable for their use as starting materials in chemical synthesis.<sup>9</sup> Biocatalysis with plasmid pKD130A indicates that these goals can be achieved. The

(4) Prentki, P.; Karch, F.; Iida, S.; Meyer, J. *Gene* **1981**, *14*, 289.

(5) (a) Zurawski, G.; Brown, K.; Killingly, K.; Yanofsky, C. *Proc. Natl. Acad. Sci. U.S.A.* **1978**, *75*, 4271. (b) Garner, C. C.; Herrmann, K. M. *J. Biol. Chem.* **1985**, *260*, 3820.

(6) While both DAH and DAHP are produced by *E. coli aroB*, DAH is produced in substantial excess. See ref 1b.

(7) Quantitation of DAH and DAHP followed the method of Gollub et al.: Gollub, E.; Zalkin, H.; Sprinson, D. B. *Methods Enzymol.* **1970**, *17A*, 349.

(8) (a) Williams, J. F.; Arora, K. K.; Longenecker, J. P. *Int. J. Biochem.* **1987**, *19*, 749. (b) Blackmore, P. F.; Williams, J. F.; MacLeod, J. K. *FEBS Lett.* **1976**, *64*, 222. (c) Williams, J. F.; Blackmore, P. F.; Duke, C. C.; MacLeod, J. K. *Int. J. Biochem.* **1980**, *12*, 339. (d) Duke, C. C.; MacLeod, J. K.; Williams, J. F. *Carbohydr. Res.* **1981**, *95*, 1.

(2) (a) Herrmann, K. M. In *Amino Acids: Biosynthesis and Genetic Regulation*; Herrmann, K. M., Somerville, R. L., Eds.; Addison-Wesley: Reading, 1983; pp 301–322. (b) Pittard, A. J. In *Escherichia coli and Salmonella typhimurium*; Niedhardt, F. C., Ingraham, J. L., Low, K. B., Magasanik, B., Schaechter, M., Umberger, H. E., Eds.; American Society for Microbiology: 1987; Vol. I, Chapter 24.

(3) (a) Josephson, B. L.; Fraenkel, D. G. *J. Bacteriol.* **1969**, *100*, 1289.

(b) Josephson, B. L.; Fraenkel, D. G. *J. Bacteriol.* **1974**, *118*, 1082.

coupled activities of transketolase and DAHP synthase, the catalytic cornerstone of multistep immobilized enzyme synthesis of DAHP, increase carbon flow into aromatic amino acid biosynthesis, leading to increased synthesis of DAH and DAHP by microbial whole cells. Equally important, this synthesis is accomplished without the need for cofactor, cosubstrates, enzyme purification, enzyme immobilization, and adenosine triphosphate regeneration demanded by multistep enzymatic synthesis.

**Acknowledgment.** Research was funded by the Searle Scholars Program, a Camille and Henry Dreyfus Teacher-Scholar Grant, and the Sloan Foundation.

(9) For examples where DAH has been used as a starting material in chemical syntheses, see: (a) Bartlett, P. A.; Satake, K. *J. Am. Chem. Soc.* **1988**, *110*, 1628. (b) Myrvold, S.; Reimer, L. M.; Pompliano, D. L.; Frost, J. W. *J. Am. Chem. Soc.* **1989**, *111*, 1861. See also ref 1a.

(10) Miller, J. H. *Experiments in Molecular Genetics*; Cold Spring Harbor Laboratory: Cold Spring Harbor, 1972.

### Hemicarcerands Permit Entrance to and Egress from Their Inside Phases with High Structural Recognition and Activation Free Energies<sup>1</sup>

Martin E. Tanner, Carolyn B. Knobler, and Donald J. Cram\*

Department of Chemistry and Biochemistry  
University of California at Los Angeles  
Los Angeles, California 90024

Received October 10, 1989

Previous papers reported that permanent guests were imprisoned during cavitation shell closures to form carceplexes,<sup>2</sup> which are closed-surface, hollow hosts that selectively incarcerate medium components (guests). This paper reports our first hemicarcerand (**1**), a carcerand<sup>2</sup> with a shell hole large enough to permit entrance and egress of molecule-sized guests (G), but which allows ordinary separations and characterizations of hosts and complexes.

Triol **2**<sup>3</sup> was isolated as byproduct (23%) in the synthesis of **3**.<sup>2a</sup> Shell closures of **2** were conducted identically with those for **3**<sup>2a</sup> (CH<sub>2</sub>ClBr-K<sub>2</sub>CO<sub>3</sub>-solvent). Hemicarceplexes **1**·G were purified by chromatography on silica gel-CHCl<sub>3</sub>/hexane and crystallized from CHCl<sub>3</sub>-CH<sub>3</sub>CN. Shell closures in (CH<sub>3</sub>)<sub>2</sub>SO gave **1**·(CH<sub>3</sub>)<sub>2</sub>SO (51%), in (CH<sub>3</sub>)<sub>2</sub>NCOCH<sub>3</sub> gave **1**·(CH<sub>3</sub>)<sub>2</sub>NCOCH<sub>3</sub> (42%), and in (CH<sub>3</sub>)<sub>2</sub>NCHO gave **1**·(CH<sub>3</sub>)<sub>2</sub>NCHO (20%). A stereoview of the crystal structure<sup>4</sup> of **1**·(CH<sub>3</sub>)<sub>2</sub>NCHO·2CH<sub>3</sub>CN·2CHCl<sub>3</sub> is shown in **4**. Note that (CH<sub>3</sub>)<sub>2</sub>NCHO is incarcerated. Each solvating CH<sub>3</sub>CN is packed between each set of four CH<sub>2</sub>CH<sub>2</sub>C<sub>6</sub>H<sub>5</sub> groups with N directed inward. Each (CH<sub>2</sub>CH<sub>2</sub>C<sub>6</sub>H<sub>5</sub>)<sub>4</sub>-CH<sub>3</sub>CN packet is capped with CHCl<sub>3</sub>. The northern hemisphere in **4** is rotated about 20° with respect to the southern. The complex has a pseudo C<sub>2</sub> axis passing through the N and O atoms of (CH<sub>3</sub>)<sub>2</sub>NCHO, whose C=O group points toward the portal.

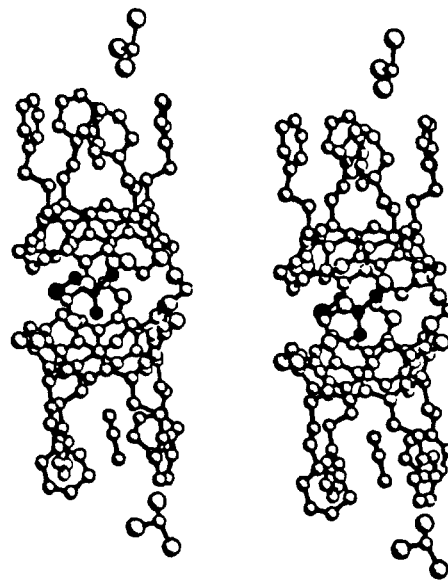
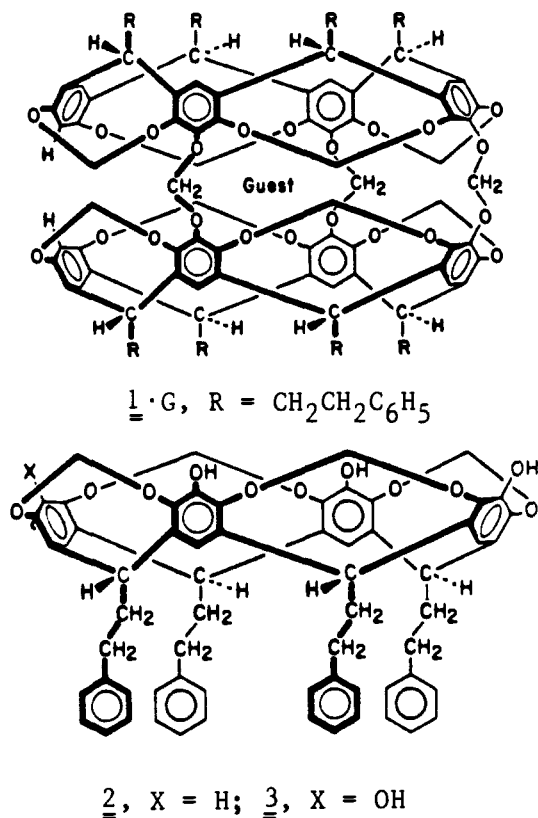
(1) We warmly thank the National Science Foundation for supporting Grant NSF CHE 8802800.

(2) (a) Sherman, J. C.; Cram, D. J. *J. Am. Chem. Soc.* **1989**, *111*, 4527-4528. (b) Cram, D. J.; Karbach, S.; Kim, Y. H.; Baczyński, L.; Kallemeyn, G. W. *Ibid.* **1985**, *107*, 2575-2576. (c) Cram, D. J.; Karbach, S.; Kim, Y. H.; Baczyński, L.; Marti, K.; Sampson, R. M.; Kallemeyn, G. W. *Ibid.* **1988**, *110*, 2554-2560.

(3) New compounds gave elemental analyses within 0.40% of theory, the expected <sup>1</sup>H NMR, and FAB MS, M + 1 ions.

(4) Crystallization of **1**·(CH<sub>3</sub>)<sub>2</sub>NCHO from CHCl<sub>3</sub>-CH<sub>3</sub>CN gave **1**·(CH<sub>3</sub>)<sub>2</sub>NCHO·2CH<sub>3</sub>CN·2CHCl<sub>3</sub>: orthorhombic, *Pbna* (standard setting *Pbcn*), *a* = 20.455 (5) Å, *b* = 20.773 (5) Å, *c* = 30.307 (8) Å, *V* = 12878 Å<sup>3</sup>, *Z* = 4 (molecule has pseudo C<sub>2</sub> symmetry, the guest is disordered about a 2-fold axis, and the chloroform is disordered about an inversion center), *R* = 0.168. Details will be published elsewhere.

Chart I



**4** (guest atoms of (CH<sub>3</sub>)<sub>2</sub>NCHO darkened)

Heating hemicarceplexes in solvents too large to become guests gave **1**<sup>5,6</sup> by expelling guests: **1**·(CH<sub>3</sub>)<sub>2</sub>SO<sup>5</sup> required 214 °C for

(5) Analyses for all elements present when summed came to 99.78-100.08%, individual analyses being within 0.40% of theory except for xenon in **1**·Xe (0.83% below 6.05% theory by thermal gravimetric analysis, summed analysis, 99.14%). Nitrogen analysis of **1** indicated that no nitrogen was present in the solid after drying at 70 °C for 12 h at 10<sup>-5</sup> Torr.

(6) When a 5 mM solution of **1** in CDCl<sub>3</sub> was saturated at 25 °C with N<sub>2</sub> (5.6 × 10<sup>-3</sup> M), <sup>1</sup>H NMR integrations of inward-turned intrahemisphere OCH<sub>2</sub>O protons of the **1**·N<sub>2</sub> produced (δ, d, 3.97, 4.12 vs **1**, δ, d, 3.93, 4.09) gave a 1:1 ratio of species, which provides a *K*<sub>a</sub> estimate of 180 M<sup>-1</sup> for **1** + N<sub>2</sub> ⇌ **1**·N<sub>2</sub>. In a similar experiment with O<sub>2</sub> (11.5 mM), a 1:2 ratio of **1**·O<sub>2</sub> to **1** was obtained, the inward OCH<sub>2</sub>O protons of **1**·O<sub>2</sub> disappearing into the base line. The Ar<sub>2</sub>CHR signals of **1** (δ, t, 4.80 and t, 4.90) were broadened and moved to δ, 5.24 and 5.38 in **1**·O<sub>2</sub>, and their integrals were used in the *K*<sub>a</sub> estimate of 44 M<sup>-1</sup> for **1** + O<sub>2</sub> ⇌ **1**·O<sub>2</sub>.